Supporting Information

Visible-Light-Driven Peroxymonosulfate Activation for Accelerating Tetracycline Removal Using Co-TiO_2 Nanospheres

Xueding Jiang [1], Jianghong Li [2], Jiesen Li [1], Weicheng Xu [1,*] and Zhang Liu [3,*]

[1] School of Environmental and Chemical Engineering, Foshan University, Foshan 528000, China; jiangxueding@fosu.edu.cn (X.J.); ljs@fosu.edu.cn (J.L.)

[2] School of Transportation and Civil Engineering, Foshan University, Foshan 528000, China; a1004269015@outlook.com

[3] Division of Environment and Sustainability, The Hong Kong University of Science and Technology, Clear Water Bay, Kowloon, Hong Kong, China

* Correspondence: weichengxu@fosu.edu.cn (W.X.); kezliu@ust.hk (Z.L.)

Contents of Supplementary material

Text S1. Chemicals
Text S2. Characterization
Text S3. TC concentration detection method by HPLC.
Text S4. Theoretical calculations.

Fig. S1. XPS survey spectra of the Co-TiO_2.
Fig. S2. N_2 sorption and desorption isotherms of TiO_2 and Co-TiO_2.
Fig. S3. (a) The degradation efficiency in different systems and (b) pseudo-second-order kinetics of TC degradation under dark condition. (Condition: catalyst doses =0.1 g/L, PMS=0.5 mM, pH = 4.8)
Fig. S4 The characterization of fresh and used Co-TiO_2 (a) XRD and (b) XPS.

Table S1. Atomic percent of elements measured by different characterization techniques.
Table S2. Textural properties of TiO_2, Co-TiO_2.
Table S3. Rate constants for reactions of quenching agents with different ROS.
Table S4. Degradation intermediate of TC detected by HPLC-MS.
Table S5. Natural population analysis (NPA) charges and calculated Fukui index (f^-, f^+, and f^0) of TC for Vis/Co-TiO_2/PMS system.

Text S1. Chemicals

Cobalt chloride hexahydrate ($CoCl_2·6H_2O$), p-benzoquinone ($C_6H_4O_2$), and L-histidine ($C_6H_9N_3O_2$) was purchased from Aladdin Industrial Corporation (Shanghai, China). Sodium chloride (NaCl), sodium sulfate anhydrous (Na_2SO_4), sodium bicarbonate ($NaHCO_3$), and methanol (CH_3OH) were provided by Sigma-Aldrich. Potassium peroxymonosulfate (PMS) triple salt ($2KHSO_5·KHSO_4·K_2SO_4$) was provided by Shanghai Macklin Biochemical Co., Ltd. Sodium borohydride ($NaBH_4$), sodium dodecyl sulfonate ($NaCl_2H_{25}SO_4$), ethylene glycol ($C_2H_6O_2$) and Rhodamine B ($C_{28}H_{31}ClN_2O_3$) was bought from Sinopharm Chemical Reagent Co. Ltd (Shanghai, China). Disodium hydrogen phosphate dodecahydrate ($Na_2HPO_4·12H_2O$), tert-butanol ($C_4H_{10}O$), ethanol (C_2H_5OH), methyl blue ($C_{37}H_{27}N_3Na_2O_9S_3$), and metronidazole ($C_6H_9N_3O_3$) were obtained from Xilong Scientific Co., Ltd. All the other chemicals were used without further purification.

Text S2. Characterization

X-ray diffraction (XRD) patterns were acquired on a Rigoku SmartLab with Cu Kα radiation (λ = 1.5406 Å) operating at 40 kV and 30 mA over a 2θ range of 10-90°. X-ray photoelectron spectroscopy (XPS) was performed on an Thermo ESCALAB 250XI spectrometer with an Al Kα X-ray source (hv = 1486.6 eV) and the C 1 speak at 284.8 eV was used to correct all of the binding energy spectra. The surface morphology of the composites was measured by scanning electron microscopy (SEM) (Quanta 400 FEG, FEI, America) equipped with an energy dispersive spectrometer (EDS) and the surface distribution was recorded using higher solution transmission electron microscopy (TEM) (Tecnai G2 F20, FEI, America). The specific surface area (SSA) and pore size distribution of the composites were determined by using a physisorption instrument (TriStar II 3020, Micromeritics, America). The electron spin resonance (ESR) spectra were obtained

on an ESR spectrometer (A300-10/12, Bruker, Germany). The concentration of the pollutant was measured using high-performance liquid chromatography (HPLC, Agilent 1260). The intermediates produced during the TC degradation process were identified by ultrahigh performance liquid chromatography combined with mass spectrometry (HPLC-MS, Thermo Fisher Scientific, Germany).

Text S3. TC concentration detection method by HPLC

The residual concentration of TC was detected by HPLC system with a detecting wavelength at 357 nm. The separation was carried out on a C-18 column with a mobile phase consisting of acetonitrile and oxalic acid (0.1 M) in the ratio of 20:80 (v/v%) at a flow rate of 1 mL/min, and acted under the temperature of 30 °C.

Text S4. Theoretical calculations

Fukui functions are an important concept in density functional theory (DFT) and have been widely used in the prediction of reaction sites for electrophilic (f^+), nucleophilic (f^-) and general free radical attacks (f^0). Specifically, Fukui functions are defined as:

$$f(r) = \left[\frac{\partial \rho(r)}{\partial N}\right]_{V(r)} \quad \text{(S1)}$$

where ρ(r) is the electron density at point r in space, N represents the number of electrons in the current system and the constant term v in the partial derivative is the external potential. In order to quantify analyze the electrophilic or nucleophilic reactivity of each atom on SMX molecule, the concept of condensed Fukui function (CFF) based on density functional theory (DFT) was proposed, which can represent the electron density distribution around the atom by the atomic population number, thus the condensed Fukui function can be explicitly calculated for three types of reactions:

Nucleophilic attack: $f_A^+ = q_N^A - q_{N+1}^A$ (S2)

Electrophilic attack: $f_A^- = q_{N-1}^A - q_N^A$ (S3)

Radical attack: $f_A^0 = (q_{N-1}^A - q_{N+1}^A)/2$ (S4)

where q^A, f, and N represent the atom charge of atom A at the corresponding state, the value of condensed Fukui function, and the number of electrons of SMX, respectively. The f value of the reaction site is usually larger than that of other regions.

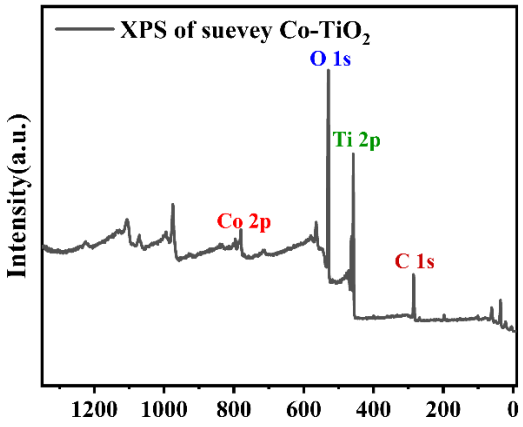


Figure S1. XPS survey spectra of the Co-TiO_2.

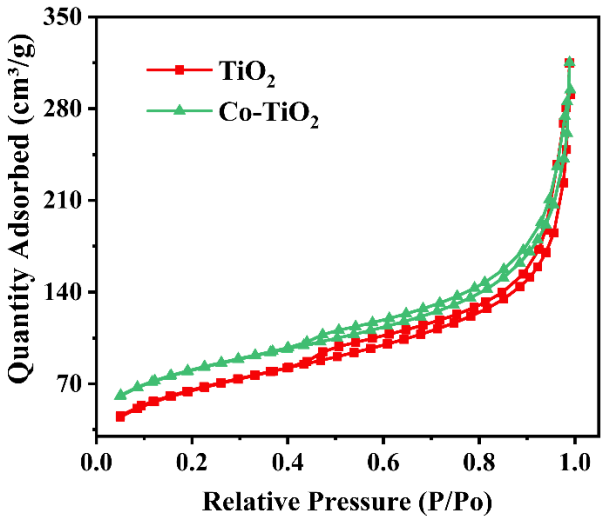


Figure S2. N_2 sorption and desorption isotherms of TiO_2 and Co-TiO_2.

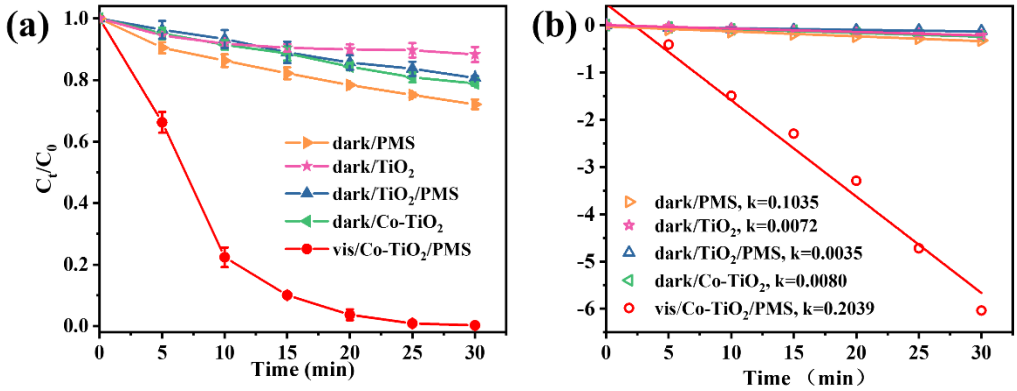


Figure S3. (a) The degradation efficiency in different systems and (b) pseudo-second-order kinetics of TC degradation under dark condition. (Condition: catalyst concentration= 0.1 g/L, PMS doses= 0.5 mM, pH = 4.8)

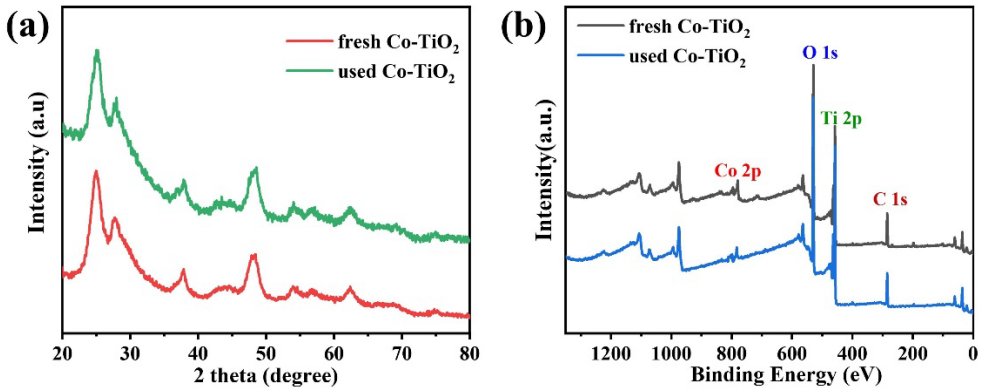


Figure S4 The characterization of fresh and used Co-TiO_2 (a) XRD and (b) XPS.

Table S1. Atomic percent of elements measured by different characterization techniques.

Technique	Ti (Atom%)	Co (Atom%)	O (Atom%)
XPS	24.89	5.42	69.69
SEM Mapping	28.74	4.60	66.66

Table S2. Textural properties of TiO_2, Co-TiO_2.

Catalyst	BET surface area (m^2/g)	Pore volume (cm^3/g)	Pore size (nm)
TiO_2	234.95	0.43	7.36
Co-TiO_2	277.60	0.45	6.43

Table S3. Rate constants for reactions of quenching agents with different ROS.

Quenching agents	Reaction rate constant (M^{-1} s^{-1})			
	•OH	$SO_4^{\bullet-}$	$O_2^{\bullet-}$	$^1O_2$
TBA	$(3.8\text{-}7.6) \times 10^8$	$(4\text{-}9.1) \times 10^5$	-	-
Methanol	9.7×10^8	2.5×10^7	-	-
p-BQ	-	-	9×10^8	
L-histidine	-	-	-	3×10^7

Table S4. Degradation intermediate of TC detected by HPLC-MS.

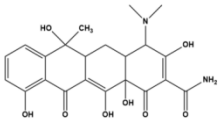
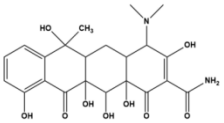
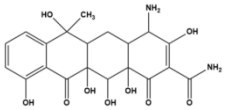
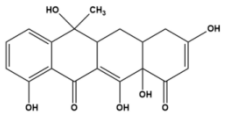
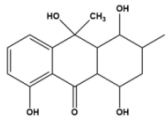
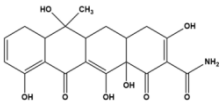
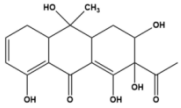
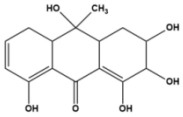
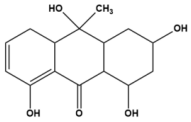
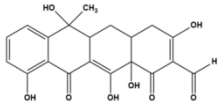
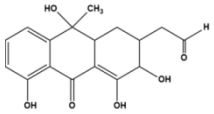
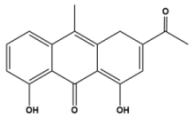
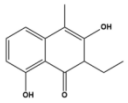
No.	Molecular formula	Measured (m/z)	Structural formula
TC	$C_{22}H_{24}N_2O_8$	445	
P1	$C_{22}H_{26}N_2O_9$	462	
P2	$C_{20}H_{22}N_2O_9$	434	
P3	$C_{19}H_{18}O_7$	358	
P4	$C_{16}H_{20}O_5$	292	
P5	$C_{20}H_{21}NO_8$	403	
P6	$C_{17}H_{20}O_7$	336	
P7	$C_{15}H_{18}O_6$	294	
P8	$C_{15}H_{20}O_5$	280	
P9	$C_{20}H_{18}O_8$	386	
P10	$C_{17}H_{18}O_6$	318	
P11	$C_{17}H_{14}O_4$	282	
P12	$C_{13}H_{14}O_3$	218	

Table S5. Natural population analysis (NPA) charges and calculated Fukui index (f^-, f^+, and f^0) of TC for Vis/Co-TiO_2/PMS system.

Atom	N-1(e/A)	N(e/A)	N+1(e/A)	f^-	f^+	f^0
C1	0.1502	0.1399	0.1336	0.0103	0.0062	0.0083
C2	0.0564	0.0295	0.0268	0.0268	0.0027	0.0148
C3	-0.0073	-0.0222	-0.0251	0.0149	0.0030	0.0089
C4	0.0777	0.0715	0.0579	0.0062	0.0136	0.0099
C5	0.1531	0.1444	0.1326	0.0086	0.0118	0.0102
C6	-0.0539	-0.0762	-0.0806	0.0223	0.0044	0.0134
C7	-0.0483	-0.0518	-0.0564	0.0035	0.0046	0.0040
C8	0.0855	0.0834	-0.0017	0.0021	0.0850	0.0436
C9	-0.0511	-0.0553	-0.0904	0.0042	0.0351	0.0197
C10	-0.0162	-0.0195	-0.0257	0.0033	0.0063	0.0048
C11	0.0894	0.0882	0.0831	0.0013	0.0050	0.0031
C12	0.1342	0.1320	-0.0071	0.0022	0.1391	0.0706
H13	0.0365	0.0283	0.0220	0.0082	0.0064	0.0073
C14	-0.0625	-0.0637	-0.0922	0.0011	0.0286	0.0148
C15	-0.0298	-0.0309	-0.0892	0.0011	0.0583	0.0297
C16	-0.0604	-0.0613	-0.0857	0.0010	0.0243	0.0127
C17	-0.0039	-0.0042	-0.0403	0.0003	0.0360	0.0182
C18	-0.0502	-0.0507	-0.0762	0.0005	0.0255	0.0130
C19	0.0847	0.0837	0.0433	0.0009	0.0404	0.0207
H20	0.0664	0.0658	0.0500	0.0006	0.0157	0.0082
H21	0.0637	0.0631	0.0398	0.0006	0.0233	0.0120
H22	0.0532	0.0526	0.0388	0.0006	0.0138	0.0072
O23	-0.2110	-0.2118	-0.2372	0.0008	0.0254	0.0131
H24	0.2099	0.2095	0.1974	0.0004	0.0122	0.0063
O25	-0.3327	-0.3373	-0.4999	0.0046	0.1626	0.0836
O26	-0.2137	-0.2194	-0.2642	0.0057	0.0448	0.0252
H27	0.1564	0.1536	0.1371	0.0028	0.0165	0.0097
O28	-0.2557	-0.2767	-0.2957	0.0210	0.0190	0.0200
C29	0.1647	0.1577	0.1556	0.0070	0.0021	0.0046
O30	-0.3954	-0.4088	-0.4122	0.0135	0.0034	0.0084
N31	-0.1264	-0.1319	-0.1339	0.0055	0.0020	0.0038
H32	0.1625	0.1585	0.1571	0.0040	0.0014	0.0027
H33	0.1475	0.1446	0.1436	0.0029	0.0010	0.0020
O34	-0.2313	-0.2386	-0.2592	0.0073	0.0207	0.0140
H35	0.1861	0.1812	0.1727	0.0049	0.0085	0.0067
O36	-0.2554	-0.2568	-0.2685	0.0013	0.0118	0.0066
H37	0.1850	0.1838	0.1758	0.0012	0.0080	0.0046
C38	-0.0854	-0.0863	-0.0915	0.0008	0.0053	0.0030
H39	0.0404	0.0393	0.0334	0.0011	0.0058	0.0035
H40	0.0446	0.0438	0.0387	0.0008	0.0051	0.0029

H41	0.0453	0.0438	0.0380	0.0015	0.0058	0.0036
N42	0.1749	-0.1013	-0.1026	0.2763	0.0013	0.1388
C43	0.0136	-0.0383	-0.0393	0.0519	0.0010	0.0265
H44	0.1048	0.0339	0.0325	0.0709	0.0014	0.0361
H45	0.1008	0.0407	0.0394	0.0601	0.0013	0.0307
H46	0.0741	0.0435	0.0424	0.0306	0.0011	0.0159
C47	0.0244	-0.0332	-0.0343	0.0575	0.0011	0.0293
H48	0.0915	0.0438	0.0427	0.0478	0.0011	0.0244
H49	0.1153	0.0347	0.0335	0.0806	0.0012	0.0409
H50	0.0880	0.0476	0.0467	0.0403	0.0009	0.0206
O51	-0.1239	-0.1378	-0.1437	0.0139	0.0059	0.0099
H52	0.2006	0.1919	0.1898	0.0086	0.0021	0.0054
H53	0.0453	0.0412	0.0285	0.0041	0.0127	0.0084
H54	0.0593	0.0423	0.0353	0.0170	0.0070	0.0120
H55	0.0861	0.0595	0.0555	0.0266	0.0040	0.0153
H56	0.0425	0.0366	0.0293	0.0059	0.0072	0.0066